FRACTURE STRESSES OF FILAMENT WOUND TUBES UNDER UNIAXIAL AND BIAXIAL LOADS

A.Amaldi and M.Marchetti
Dipartimento Aerospaziale, Università "La Sapienza"
Rome, Italy

Abstract

In this paper are presented the experimental and numerical results obtained by investigating the behaviour of angle-ply carbon/epoxy laminated composites when subjected to uniaxial and biaxial loads. Specimens are filament wound cylindrical tubes with different angles θ of fiber deposition with respect to the tube's longitudinal axis. About forty specimens with $[\pm 35]_s$, $[\pm 55]_s$ and $[\pm 75]_s$ patterns have been tested on the whole. Both uniaxial and biaxial loads have been carried out up to specimens' failure using an hydraulic circuit and an axial testing machine to apply internal pressure and tensile or compressive loads respectively, in order to investigate the effect of winding angle θ on the failure strength of the specimens. Three dimensional finite element and thin shell analyses have been applied to the problem using different failure criteria in order to predict specimens' failure for a comparison with experimental results.

1. Introduction

Filament winding tecnique provides a means of producing high fibre volume fraction composites in which laminae can be stacked using different orientations, different fibre types and matrix systems according to the loading conditions[1,2]. Practical filament wound components and structures are usually subject to complex loads involving multiaxial stress systems. The rising importance of advanced composites industry has increased interest in the development of satisfactory standard test methods to measure the properties of these materials. The individual lamina can be characterized by testing unidirectional laminates, and the data obtained can be used to investigate laminate properties. Different methods exist for theoretical stress analysis and design of filament wound components. Netting analysis[1,3] provides a simply but limited design method. More general methods are applicable for the analysis of fibre reinforced laminates[4-7], where the characterization of each lamina requires more elastic properties than conventional isotropic materials. Nine independent stiffness components, and a large number of strength and strain properties, are required to fully characterize a material with orthotropic symmetry, while for a transversely isotropic material the independent stiffness components are reduced to five. The analysis of thin plate components is currently considered, so that only in-plane properties are needed. In this work a first approach to the study of laminate behaviour when subject to biaxial stresses is presented. Tubular specimens have been adopted in order to avoid the edge-effect, due to the stress singularities at the edge of laminates[8-11] . Furthermore internal pressure can be easily applied to cylindrical specimens, in order to obtain biaxial loading conditions when combined with axial load. Specimens used in this work were not provided with end-reinforcements, often used in previous works[12-14] in order to prevent the end-effect problems due to the concentration of stresses in the gripping regions. Thus experimental results are probably affected by the end-effects. The numerical investigation has been carried out using the finite element system CASTEM 2000. The application of different failure criteria allows to obtain failure envelopes that give predictions of laminate strength at different biaxial stress conditions. The comparison of theoretical results with experimental data can serve to estabilish failure criteria that give best predictions of the laminate strength properties.

2. Assumptions and basic equations

The study of laminate behaviour is based on classical lamination theory[4]. Each orthotropic lamina (Fig.1) is characterized by the transformed reduced stiffness matrix $\overline{Q}$, relative to the x-y reference axes in the plane of the lamina, whose components depend on Young's moduli E_1 and E_2, respectively in fibres and matrix directions and assumed equal in tension and compression, on shear modulus G_{12}, on Poisson's ratio ν_{12} and on the angle θ of rotation between x-y reference axes and 1-2 lamina principal axes.

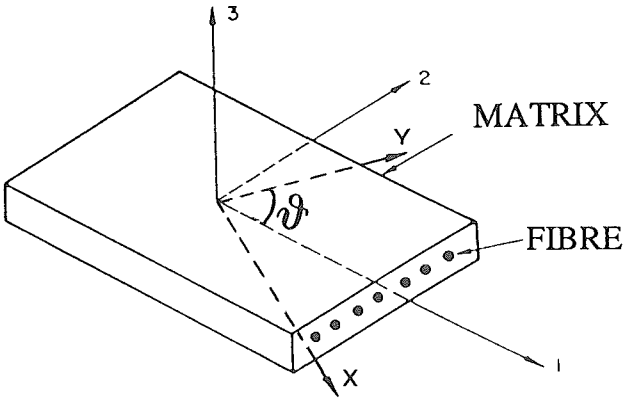

Fig.1 Schematic of orthotropic lamina geometry

The stress-strain relations in x-y coordinates are:

$$\begin{Bmatrix}\sigma_x\\ \sigma_y\\ \tau_{xy}\end{Bmatrix}=\begin{bmatrix}\overline{Q}_{11} & \overline{Q}_{12} & \overline{Q}_{13}\\ \overline{Q}_{21} & \overline{Q}_{22} & \overline{Q}_{23}\\ \overline{Q}_{31} & \overline{Q}_{32} & \overline{Q}_{33}\end{bmatrix}\begin{Bmatrix}\varepsilon_x\\ \varepsilon_y\\ \gamma_{xy}\end{Bmatrix} \quad (1)$$

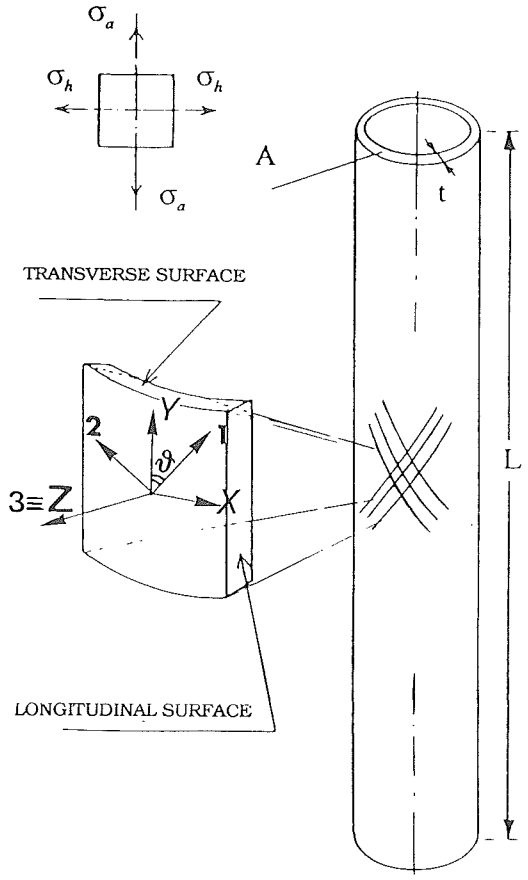

Fig.2 Definition of stress components for tubular specimen

A laminate is obtained by the superposition of n laminae, and when it is subject to a general state of stresses in the x-y plane, the resultants forces and moments are related to the laminate middle surface strains and curvatures as follows:

$$\begin{Bmatrix} N_x \\ N_y \\ N_{xy} \\ M_x \\ M_y \\ M_{xy} \end{Bmatrix} = \begin{bmatrix} A_{11} & A_{12} & A_{16} & B_{11} & B_{12} & B_{16} \\ A_{21} & A_{22} & A_{26} & B_{21} & B_{22} & B_{26} \\ A_{61} & A_{62} & A_{66} & B_{61} & B_{62} & B_{66} \\ B_{11} & B_{12} & B_{16} & D_{11} & D_{12} & D_{16} \\ B_{21} & B_{22} & B_{26} & D_{21} & D_{22} & D_{26} \\ B_{61} & B_{62} & B_{66} & D_{61} & D_{62} & D_{66} \end{bmatrix} \begin{Bmatrix} \varepsilon_x^0 \\ \varepsilon_y^0 \\ \gamma_{xy}^0 \\ k_x \\ k_y \\ k_{xy} \end{Bmatrix} \quad (2)$$

where:

$$A_{ij} = \sum_{k=1}^{n} (\overline{Q}_{ij})_k (z_k - z_{k-1}) \quad (3)$$

$$B_{ij} = \frac{1}{2} \sum_{k=1}^{n} (\overline{Q}_{ij})_k (z_k^2 - z_{k-1}^2) \quad (4)$$

$$C_{ij} = \frac{1}{3} \sum_{k=1}^{n} (\overline{Q}_{ij})_k (z_k^3 - z_{k-1}^3) \quad (5)$$

for a n-layered laminate.

In the present work a number of angle-ply, symmetric and balanced pattern $[\pm\theta]_s$ laminates were studied (n=4). General conditions of biaxial stress were obtained by simultaneously applying internal pressure P and axial load F_a to the tubular specimens. As a consequence an axial stress σ_a and a circumferential stress (or hoop stress) σ_h are assumed to act in the laminate transverse and longitudinal directions respectively (Fig.2).

3. Numerical approach

The numerical investigation, based on three dimensional finite element and thin shell analyses, has been carried out in collaboration with ENEA (Ente Nuove Tecnologie Energia ed Ambiente, "La Casaccia", Rome) using CEA's (Commissariat à l'Energie Atomique, Saclay, France) general purpose finite element system CASTEM 2000[15-18]. Different failure criteria have been adopted in order to predict specimens' failure under biaxial loading conditions at different stress ratios $R = \sigma_h/\sigma_a$. For each one of the three classes of $[\pm\theta]_s$ laminates considered, a failure envelope in the $\sigma_h - \sigma_a$ plane is obtained numerically by the use of a failure criterion. Each failure envelope predicts, relatively to that particular laminate and failure criterion adopted, the loading level at which stresses first exceed the material basic failure strengths of the laminate for different ratios R . The failure criteria adopted in this work were the linear maximum-stress and maximum-strain criteria, and the quadratic Tsai-Wu, Hoffmann and Tsai-Hill criteria. The analysis presented above has been carried out as represented in the flow diagram of Fig.3. Once a ply has failed for a certain loading value (first-ply failure) the strength properties of the laminate are changed, in the sense that the failed lamina is assumed to give no more contribute to the

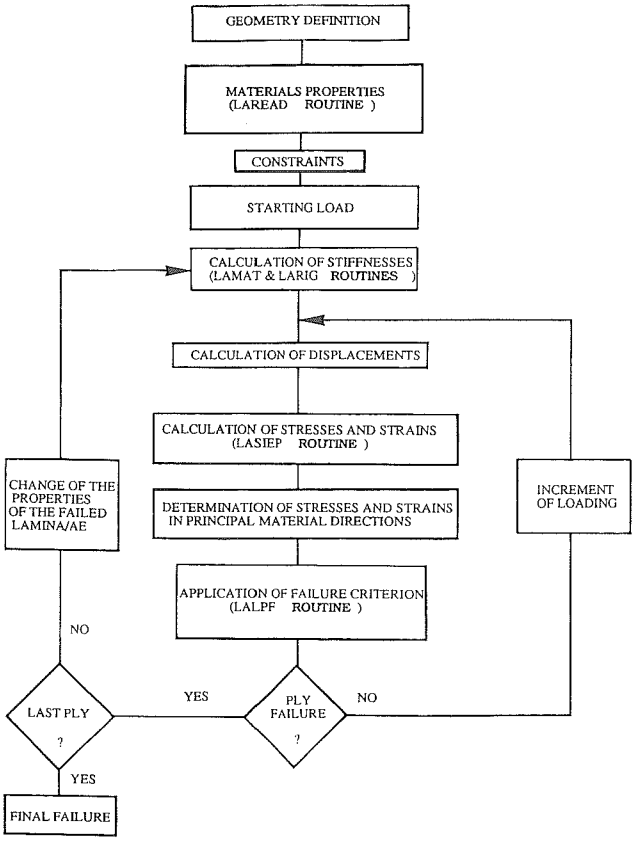

Fig.3 Flow diagram for the computer programme used to calculate theoretical failure envelopes

strength of the laminate. Then calculations restart and, if no other lamina has failed, load is incremented until final failure (last-ply failure). Because of the geometrical and loading axialsimmetry of the cylindrical structure examined, here only one failure envelope appears, as first and final failure are coincident. Among the various hypothesis on which lamination theory is based, the assumption of shear linearity must be underlined, as composites often have a marked non-linear behaviour in shear. In addition more accurate predictions of laminate strength could be obtained representing into a progressive failure criterion the stiffness changes that occur in a ply when loaded, in spite of roughly eliminating any resistance of the failed lamina.

4. Experimental approach

Specimens

Specimens, manufactured by Barwell International Ltd (U.K.), are filament wound carbon fibre/epoxy resin tubes with interwoven pattern $[\pm\theta]_s$, with θ being 35°, 55° or 75°. EXAS HS11 carbon fibres and a CIBA GEIGY epoxy resin system (HK 2954 and LY564-1) have been used in a wet winding process with 60% of fibre volume fraction. All the tubes have 42 mm nominal internal diameter and are 250 mm long. The wall thicknesses, measured at forty points on the surface of each specimen, are given in table 1 for each class of tubes. The mechanical properties of materials are listed in tables 2 and 3.

Table 1 - Thicknesses of specimens

LAMINATE PATTERN	NOMINAL AVERAGE THICKNESS (mm)
$[\pm35]_s$ INTERWOVEN	1.89
$[\pm55]_s$ INTERWOVEN	1.71
$[\pm75]_s$ INTERWOVEN	1.78

Table 2 - Elastic properties of materials

E_1 (GPa)	E_2 (GPa)	ν_{12}	G_{12} (GPa)
140	10	0.3	4.8

Table 3 - Lamina strength properties

X_T(MPa)	X_C(MPa)	Y_T(MPa)	Y_C(MPa)	S(MPa)
2500	1400	55	270	110

Experimental Apparatus and Procedure

Grips have been designed and manufactured for loading the tubular specimens. Each grip consists of a steel plug and two jaws. Plugs are inserted in the upper and lower ends of the specimen, and jaws are clamped externally (Fig.4). The upper grip is provided with a hole that is connected with a butyl liner in order to give pressure inside the specimen. Tests have been carried out using an hydraulic circuit to apply pressure load and a Schenk M100 testing machine to apply axial load. A flow regulator allows to change pressure gradually up to 100 Bars with the hydraulic circuit, that has been used to obtain biaxial loading conditions by simultaneously applying axial load to the specimens while keeping constant the ratio of applied forces (i.e. the ratio R). Besides a 700 Bars hand-pump, not permitting a fine regulation of pressure changes, has been used for loading specimens with internal pressure only. With this last loading procedure, carried out on unlined specimens since pressures reached were too high for the liner resistance, two different stress conditions could be obtained depending upon whether grips were restrained each other or not (Figs.5,6).

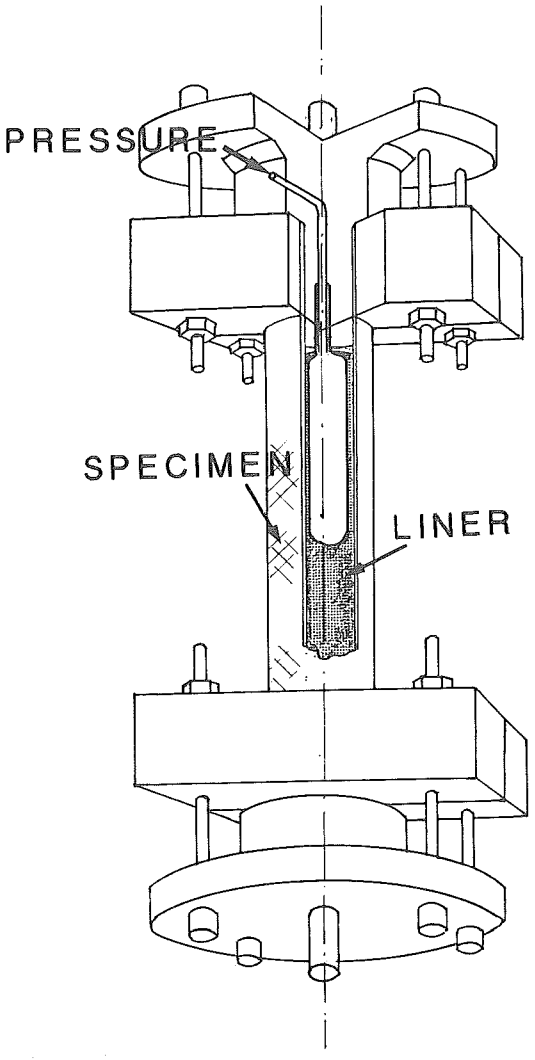

Fig.4 Schematic of tubular specimen with end grips and liner

5. Discussion and concluding remarks

By carrying internal pressure and axial load up to failure at different stress ratios R, experimental strength data have been obtained for the three classes of $[\pm\theta]_s$ tubular specimens considered. Theoretical failure envelopes, obtained as previously described using different failure criteria, are compared in Figs.7-9 to the experimental results obtained with uniaxial and biaxial tests carried out on $[\pm35]_s$, $[\pm55]_s$ and $[\pm75]_s$ specimens respectively. The points of failure obtained applying netting analysis are represented with an asterisk, with the corresponding stress ratio given in brackets. Biaxial-test results couldn't be obtained all over the range of stress ratios R, because a fine regulation of the

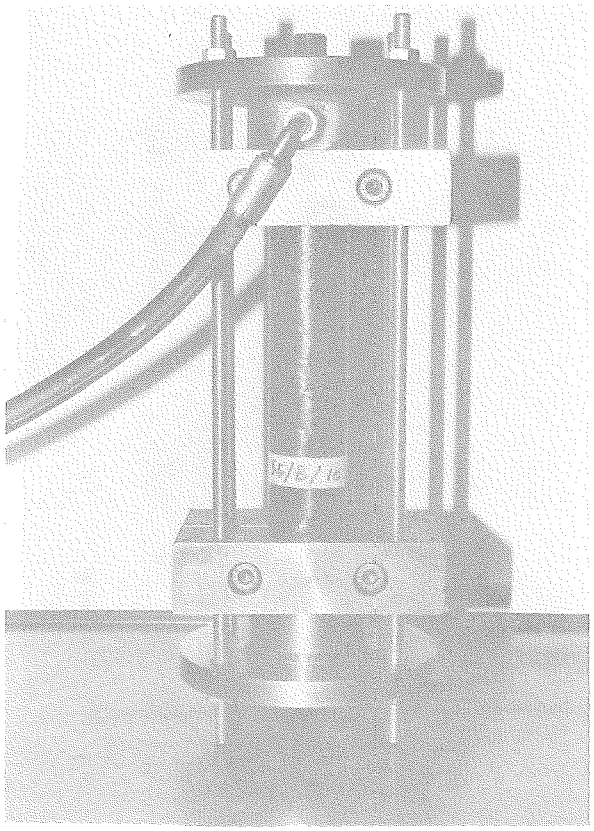

Fig.5 Internal pressure testing with restrained ends of the tube (no axial strain allowed)

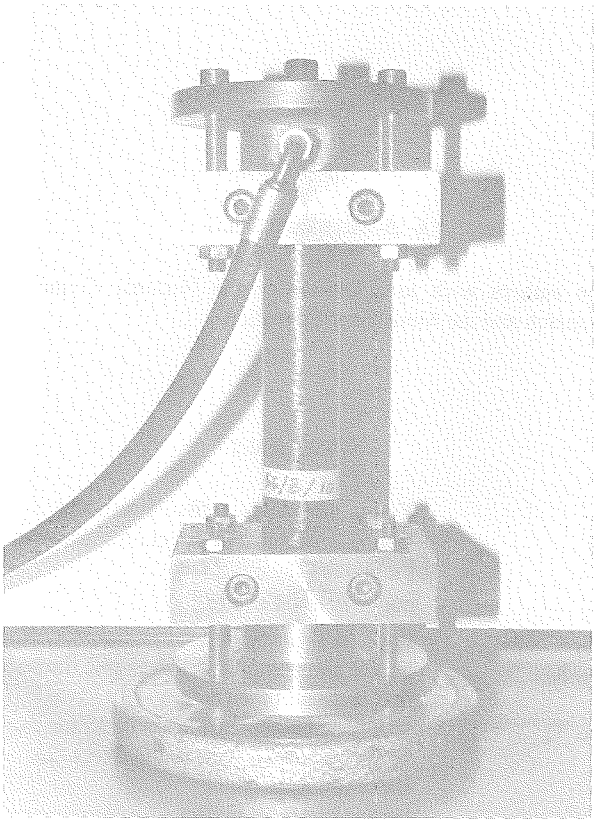

Fig.6 Internal pressure testing with R=2 (closed-ends condition)

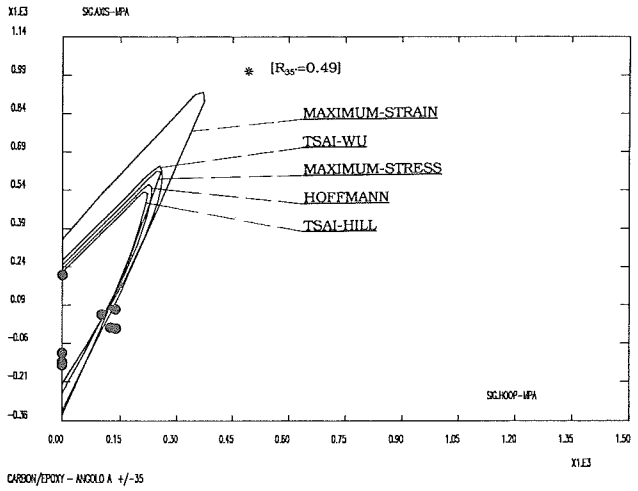

Fig.7 Failure envelopes for $[\pm 35]_s$ with experimental data

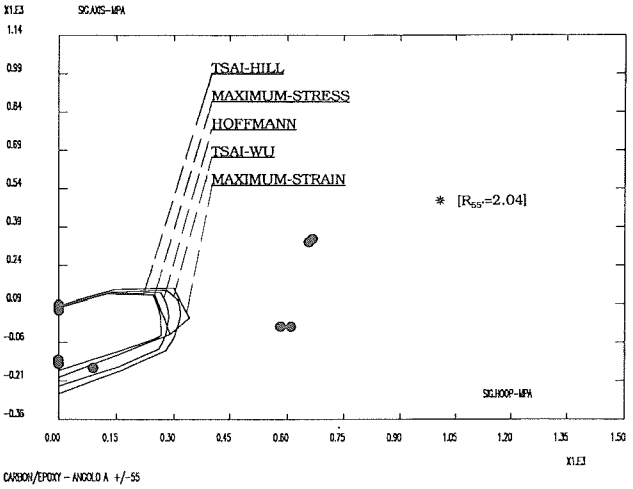

Fig.8 Failure envelopes for $[\pm 55]_s$ with experimental data

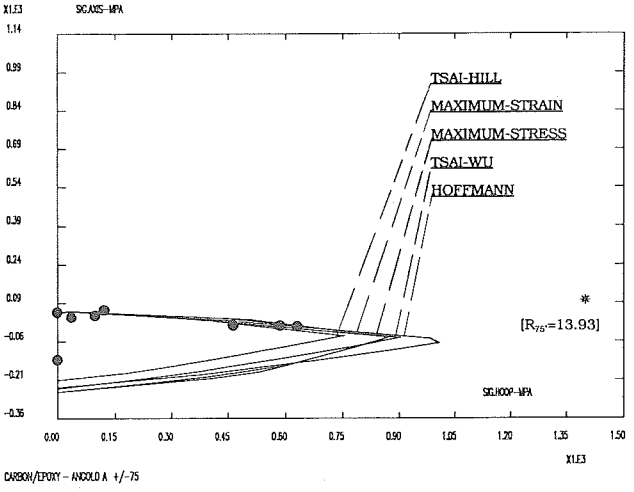

Fig.9 Failure envelopes for $[\pm 75]_s$ with experimental data

pressure loading ramp would have been necessary up to 700-800 Bars and not only up to 100 Bars. Anyway some relevant remarks must be pointed out before commenting Figs.7-9. As a matter of fact specimens used in this work were not provided with end-reinforcements, and almost all the tubes tested fractured at the ends (see Figs. 10 and 11 for example), while only few specimens fractured in the middle region (Fig.12). It follows that the experimental results obtained probably give underestimated values of the effective strength of the laminate, because failure of specimens is probably due to the concentration of stresses associated with end-gripping and pressure-sealing regions. At the same time, however, applying our computer programme to similar problems investigated in previous works, it predicted failure envelopes that were much conservative compared to those obtained for example in reference 19, where the main differences were the allowance for shear non-linearity and the application of a progressive failure criterion. As a consequence of the considerations given above, Figs.7-9 could be undeceiving, because the experimental data are probably underestimated and numerical predictions are too conservative. The design of end-reinforcements is then absolutely required in order to obtain more accurate experimental results on tubular specimens. Besides more realistic failure envelopes could be predicted numerically taking into account shear non-linearity, and developing a suitable progressive failure criterion in the computer programme. Work is in progress in order to improve the quality of both experimental and numerical results.

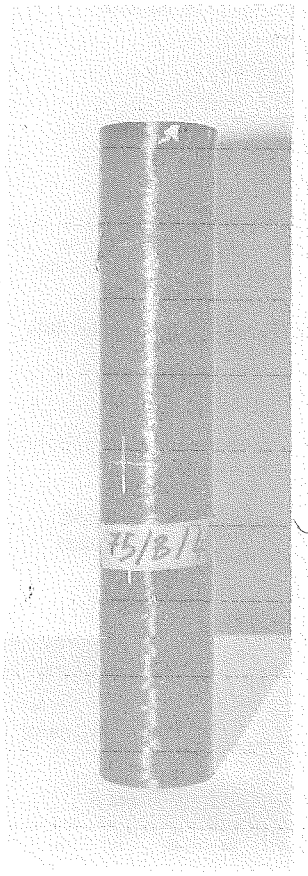

Fig.10 $[\pm 75]_s$ specimen fractured in the gripping region under biaxial stress (R=1)

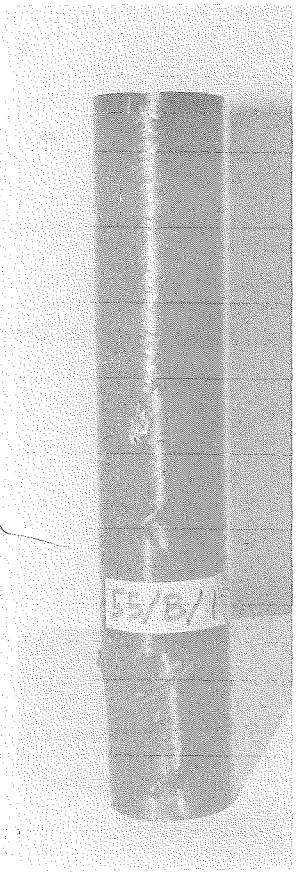

Fig.11 $[\pm 55]_s$ specimen fractured in the gripping region under axial compression

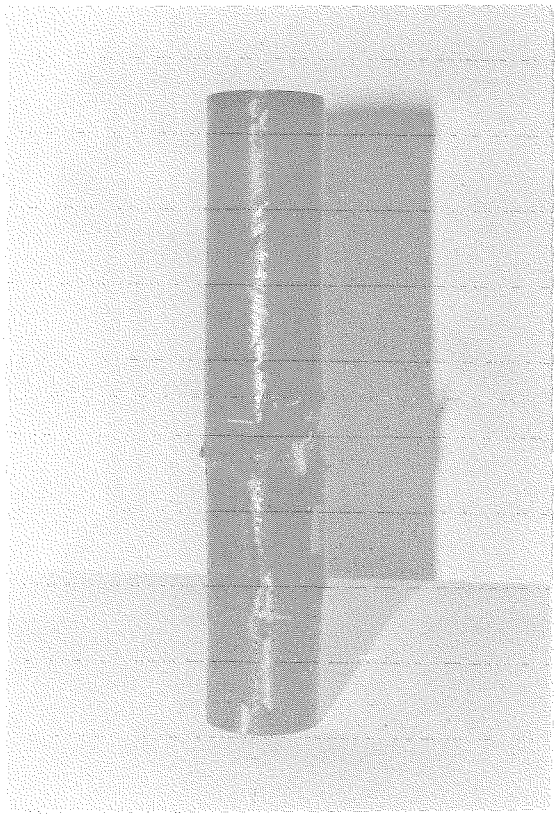

Fig.12 $[\pm 55]_s$ specimen fractured in the middle region under internal pressure (restrained as in Fig.5)

Acknowledgements

The authors wish to acknowledge the National Council of Research and the Ministry of Education.

Nomenclature

E_1	Young's modulus in fibre direction (1)
E_2	Young's modulus in direction transverse to the fibres (2)
ν_{12}	major Poisson's ratio
G_{12}	in-plane shear modulus
X_T, X_C	tensile and compressive strengths measured in direction of the fibres
Y_T, Y_C	tensile and compressive strengths measured in direction transverse to the fibres (2)
S	shear strength
$\sigma_x, \sigma_y, \tau_{xy}$	lamina in-plane stresses
$\varepsilon_x, \varepsilon_y, \gamma_{xy}$	lamina in-plane strains
$\overline{Q}_{ij}$	transformed reduced stiffnesses

N_x, N_y, N_{xy}	resultant forces on laminate
M_x, M_y, M_{xy}	resultant moments on laminate
$\varepsilon_x^0, \varepsilon_y^0, \gamma_{xy}^0$	laminate middle-surface strains
k_x, k_y, k_{xy}	laminate middle-surface curvatures
A_{ij}	extensional stiffnesses
B_{ij}	coupling stiffnesses
C_{ij}	bending stiffnesses
F_a	axial load
P	internal pressure
A	cross-sectional area of cylinder
r	radius of cylinder
t	thickness of cylinder
$\sigma_a = F_a/A$	axial stress in cylinder under axial load
$\sigma_h = Pr/t$	hoop stress in cylinder under internal pressure
R	biaxial stress ratio

References

1. Rosato,D.V. and Grove,C.S.Jr Filament Winding: it's Development, Manufacture, Applications and Design, Interscience Publishers, 1964.

2. Di Vita,G., Marchetti,M., Moroni,P. and Perugini,P. A Complete Procedure to Design Filament Wound Structures, Composite Manufacturing, ed. Butterworth Heinemann, U.K., 1992, in press.

3. Bishop,P.H.H. Predicting Mechanical Properties of Fibre Composites in Glass Reinforced Plastics, ed.B.Parkyn (ILIFFE Books, London, U.K., 1970), chapter 13, pp.169-189.

4. Jones,R.M. Mechanics of Composite Materials, ed. Mc Graw-Hill Kogakusha, LTD.

5. Tsai,S.W. Strength Theories of Filamentary Structures, in Schwartz,R.T. e Schwartz,H.S. (eds.) Fundamental Aspects of Fiber Reinforced Plastic Composites, Wiley Interscience, New York, pp.3-11, 1968.

6. Tsai,W. and Hahn,H.T. Introduction to Composite Materials, Westport: Technomic, 1980.

7. Handbook of Composites, Vol.3, Failure Mechanics of Composites, published by Sui,G.C. e Skudra,A.M., 1985.

8. Swanson,S.R. and Trask,B.C. An Examination of Failure Strength in [0/60] Laminates under Biaxial Stress, Composites, Vol.19 (n°5), pp.400-406, 1988.

9. Guess,T.R. Biaxial Testing of Composite Cylinders: Experimental-Theoretical Comparison, Composites, Vol.11 (n°3), pp.139-148, 1980.

10. Guess,T.R. and Gerstle,F.P.Jr. Deformation and Fracture of Resin Matrix Composites in Combined Stress States, Journal of Composite Materials, Vol.11, pp.146-163, 1977.

11. Icardi,U. and Manuello,A. Some Considerations Regarding the Edge Stress Problem of Laminates by Finite Elements, Computers and Structures, vol.40, n°3, pp.581-597, 1991.

12. Swanson,S.R.,Christoforou,A.P. and Colvin,G.E.Jr. Biaxial Testing of Fiber Composites Using Tubular Specimens, Experimental Mechanics, pp.238-243, sept.1988.

13. Toombes,G.R.,Swanson,S.R. and Cairns,D.S. Biaxial Testing of Composite Tubes, Experimental Mechanics, Vol.25, pp.186-192, 1985.

14. Highton,J. and Soden,P.D.W. End Reinforcement and Grips for Anisotropic Tubes, Journal of Strain Analysis, vol.17, n°1, 1982.

15. Castem 2000 - Notice 1991, CEA, Saclay.

16. Castem 2000 - Elèment Coque Mince, Excentrè, Orthotrope, Rapport DEMT 89/410, Départment des Etudes Méchaniques et Thermiques, CEA, Saclay.

17. Castem 2000 - Manuali Utente, ENEA, Rome.

18. Miliozzi,A. Un Set di Procedure per l'Analisi di Laminati Compositi, Rapp. ENEA-CASTEM 2000, in press.

19. Eckold,G.C.,Leadbetter,D.,Soden,P.D. and Griggs,P.R. Lamination Theory in the Prediction of Failure Envelopes for Filament Wound Materials Subjected to Biaxial Loading, Composites, Vol.9 (n°4), pp.243-246, 1978.

20. Amaldi,A., Giannuzzi,M., Marchetti,M. and Miliozzi.,A. Numerical Simulation and Experimental Results of Filament Wound CFRP Tubes Tested under Biaxial Load, proc. of the "International Symposium on Advanced Materials for Lightweight Structures", 25-27 March 1992, ESA, ESTEC, in press.